Article

Current Biology

Post-embryonic remodeling of the *C. elegans* motor circuit

Highlights

- Serial EM reconstitution of post-embryonic motor circuit maturation
- Post-embryonic motor circuit maturation eliminates wiring asymmetry
- Programmed rewiring gradually and sequentially transforms circuit structure
- Preparatory rewiring facilitates structural maturation without functional disruption

Authors

Ben Mulcahy, Daniel K. Witvliet, James Mitchell, ..., Andrew D. Chisholm, Jeff W. Lichtman, Mei Zhen

Correspondence

mulcahy@lunenfeld.ca (B.M.), meizhen@lunenfeld.ca (M.Z.)

In brief

Animals employ strategies to maintain behaviors as circuits remodel. The *C. elegans* motor circuit expands and rewires while maintaining an undulatory motor pattern. Mulcahy et al. uncover several developmental strategies by EM reconstruction of the motor circuit across development.

Mulcahy et al., 2022, Current Biology *32*, 4645–4659
November 7, 2022
https://doi.org/10.1016/j.cub.2022.09.065

CellPress

Current Biology

CellPress

Article

Post-embryonic remodeling of the *C. elegans* motor circuit

Ben Mulcahy,[1,7,*] Daniel K. Witvliet,[1,5] James Mitchell,[2] Richard Schalek,[3] Daniel R. Berger,[3] Yuelong Wu,[3] Doug Holmyard,[1] Yangning Lu,[1,6] Tosif Ahamed,[1] Aravinthan D.T. Samuel,[2] Andrew D. Chisholm,[4] Jeff W. Lichtman,[3] and Mei Zhen[1,8,9,*]

[1]Lunenfeld-Tanenbaum Research Institute, Mount Sinai Hospital, Toronto, ON M5G 1X5, Canada
[2]Department of Physics, Center for Brain Science, Harvard University, Cambridge, MA 02138, USA
[3]Department of Molecular and Cellular Biology, Center for Brain Science, Harvard University, Cambridge, MA 02138, USA
[4]Division of Biological Sciences, University of California, San Diego, La Jolla, CA 92093, USA
[5]Present address: Coursera, Toronto, ON M5C 2L7, Canada
[6]Present address: McGovern Institute for Brain Research, Massachusetts Institute of Technology, Cambridge, MA 02139, USA
[7]Twitter: @Ben_Mulcahy
[8]Twitter: @zhenlab_Toronto
[9]Lead contact
*Correspondence: mulcahy@lunenfeld.ca (B. M.), meizhen@lunenfeld.ca (M. Z.)
https://doi.org/10.1016/j.cub.2022.09.065

SUMMARY

During development, animals can maintain behavioral output even as underlying circuitry structurally remodels. After hatching, *C. elegans* undergoes substantial motor neuron expansion and synapse rewiring while the animal continuously moves with an undulatory pattern. To understand how the circuit transitions from its juvenile to mature configuration without interrupting functional output, we reconstructed the *C. elegans* motor circuit by electron microscopy across larval development. We observed the following: First, embryonic motor neurons transiently interact with the developing post-embryonic motor neurons prior to remodeling of their juvenile wiring. Second, post-embryonic neurons initiate synapse development with their future partners as their neurites navigate through the juvenile nerve cords. Third, embryonic and post-embryonic neurons sequentially build structural machinery needed for the adult circuit before the embryonic neurons relinquish their roles to post-embryonic neurons. Fourth, this transition is repeated region by region along the body in an anterior-to-posterior sequence, following the birth order of neurons. Through this orchestrated and programmed rewiring, the motor circuit gradually transforms from asymmetric to symmetric wiring. These maturation strategies support the continuous maintenance of motor patterns as the juvenile circuit develops into the adult configuration.

INTRODUCTION

The nervous system is built in embryos but continues to expand and remodel after birth.[1–3] Postnatal changes are associated with changes in body size, body plan, behavior, and habitat of the maturing animal.[4–7] During postnatal development, as circuits remodel, animals may update behaviors or compensate structural changes to maintain behaviors.

The *C. elegans* motor circuit grows dramatically during post-embryonic stages.[2,3,8] A newly hatched larvae (L1) has 22 ventral cord motor neurons, adding 53 more by early second larva (L2) stage (Figure 1A). Both L1 larvae and adults exhibit dorsoventral undulatory patterns.[9]

Motor neurons wire differently between newborn L1 larvae and adults.[10,11] L1 motor neurons belong to three classes. Two sets of cholinergic excitatory motor neurons (eMNs), DA1–9 and DB1–7, contract dorsal muscles. One set of GABAergic inhibitory motor neurons (iMNs), DD1–6, relax ventral muscles. Members of the same class distribute along the cord; neighboring members form tiled neuromuscular output. An eMN that contracts dorsal muscles also synapses onto an iMN that relaxes opposing ventral muscles, thereby forming a dorsal-bending circuit (Figure 1B).

Embryonic and post-embryonic motor neurons inter-wire to form the adult motor circuit.[9,12,13] The 53 post-embryonic motor neurons add four new classes for body bending: three sets of eMNs contract ventral (VA1–12 and VB1–11) or dorsal (AS1–11) muscles; one set of iMNs (VD1–13) relaxes ventral muscles. With the set of embryonic iMNs (DD1–6) rewired to relax dorsal muscles, the adult motor circuit forms two subcircuits: eMNs that contract muscles on one side synapse onto iMNs that relax muscles on the opposite side, forming dedicated dorsal and ventral bending circuits[9,12–16] (Figure 1B).

Therefore, post-embryonic development eliminates L1 dorsoventral wiring asymmetry. This requires the juvenile circuit to integrate post-embryonic motor neurons and rewire embryonic motor neurons. Strikingly, the embryonic DD iMNs fully reverse their neurite polarity during rewiring,[10,17] with ventral and dorsal neurites acquiring different synaptic partners in L1 and adult.[10,11,14]

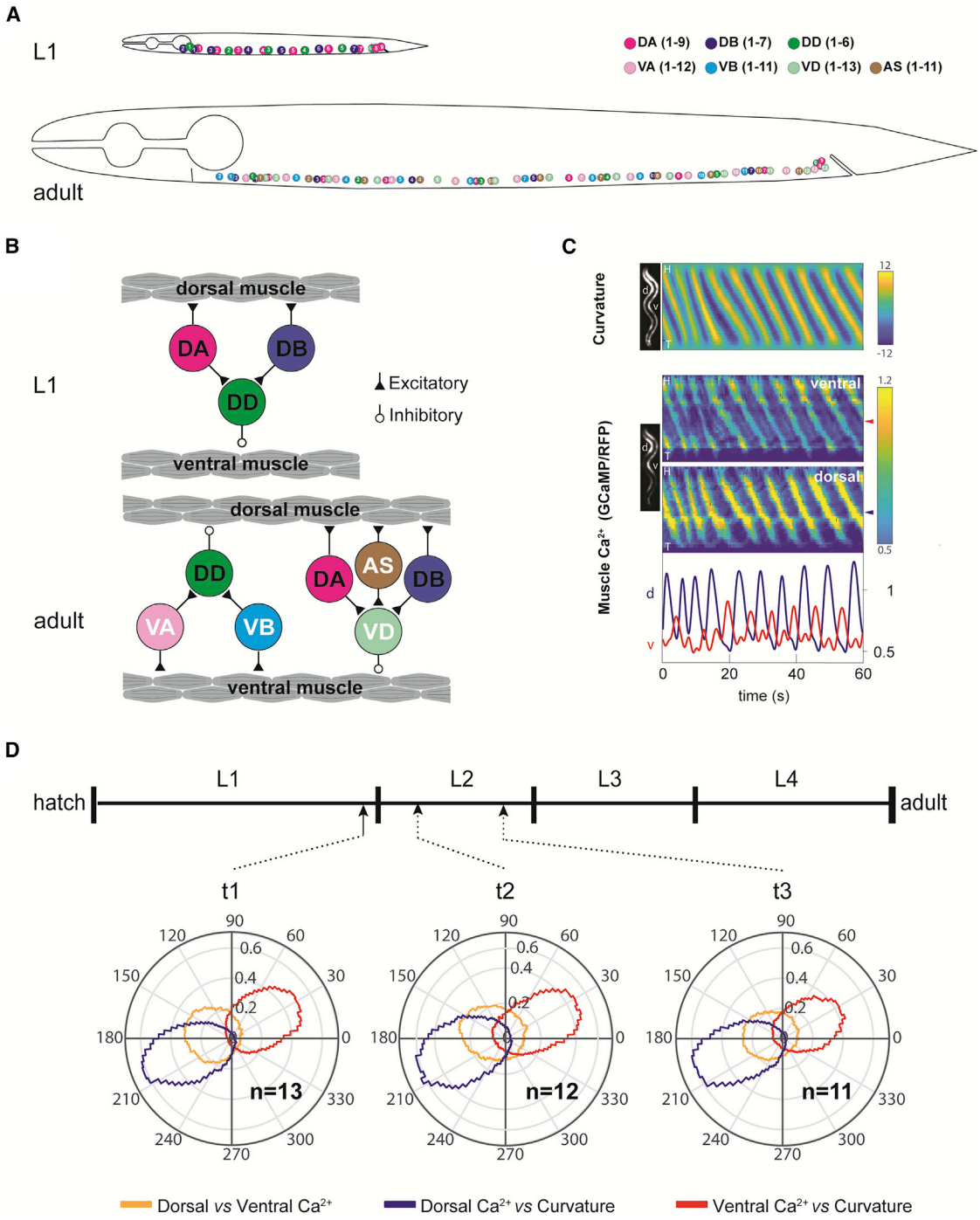

Figure 1. *C. elegans* larvae maintain coordinated motor output as the motor circuit matures

(A) Schematics of body motor neuron soma in newborn L1 and adult (not to scale, VC not shown).

(B) Wiring diagram between motor neuron classes and body wall muscles in L1 and adult.

(C) Representative kymographs of a freely crawling larva (t2 in D) expressing calcium reporter in body wall muscles. Top: body curvature over time. Segments 1 and 30, respectively, denote the head and tail. Middle: calcium signals in ventral and dorsal muscles along the body. Bottom: example calcium signals of the mid-body ventral (blue) and dorsal (red) muscles (segment 18).

(D) Polar histograms of phase differences along the body (segments 11–30), between muscle activities and curvature, at the onset, middle, and end of rewiring (n = 11–13 animals).

See also Data S1.

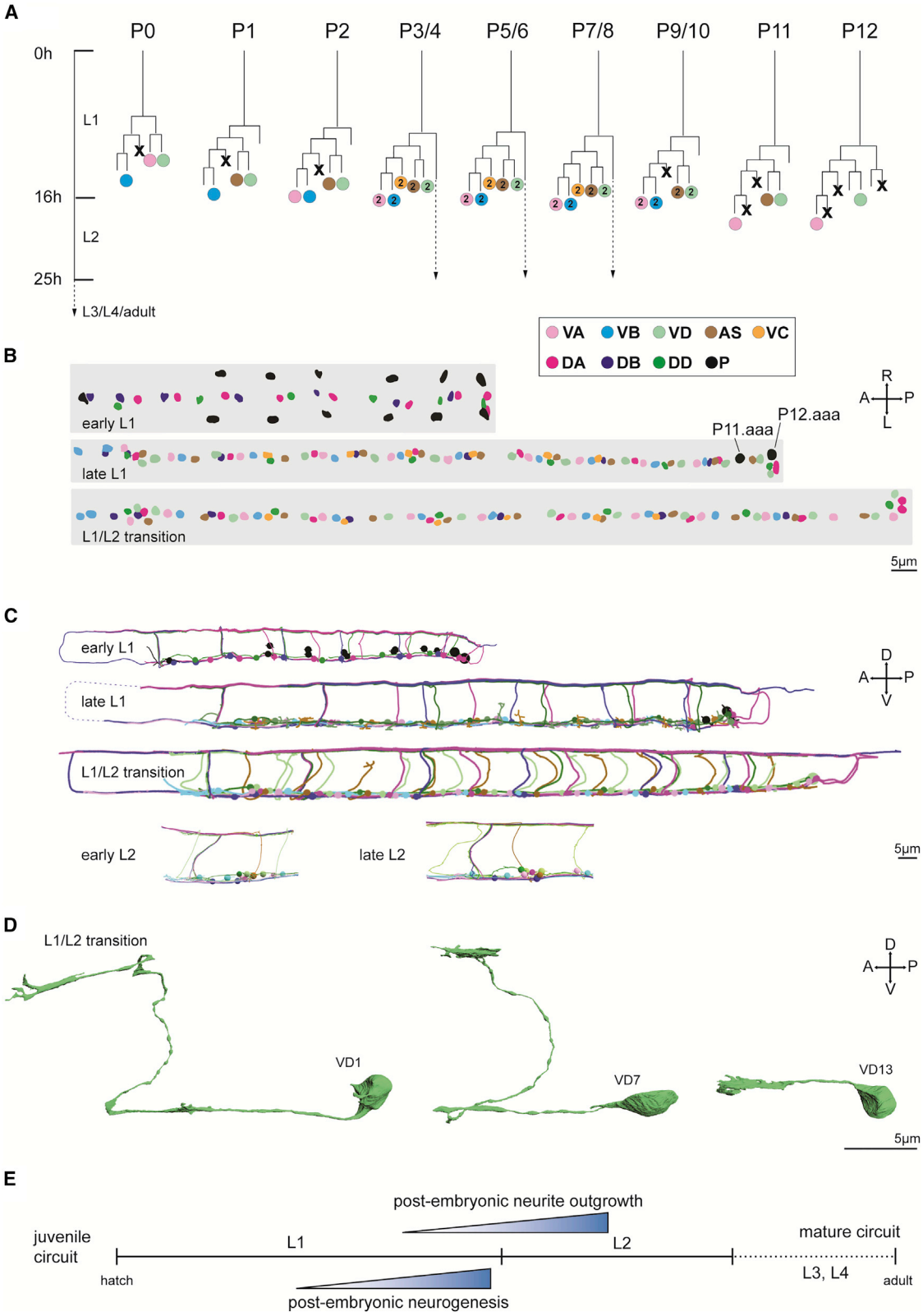

Figure 2. Post-embryonic motor neuron birth and growth follows a stereotyped process

(A) The lineage tree of post-embryonic motor neurons. Each horizontal line denotes one stereotyped cell division event. Only neuronal progenies are denoted. X: apoptosis. Adapted from Sulston et al.[2]

(legend continued on next page)

How might post-embryonic expansion and rewiring take place without changing motor patterns? We addressed this question with two studies. In one study,[11] we explained how newborn L1 larvae generate adult-like body bends with only a dorsal bending circuit. Without a dedicated circuit for ventral bending, L1 ventral bending occurs through extrasynaptic potentiation of ventral muscles and anti-phasic entrainment to the dorsal bending circuit.[11]

With different mechanisms in place to produce similar motor patterns in L1 larvae and adults, it is possible for developing larvae to maintain their motor output. Here, we examined how the motor circuit transforms through synapse-resolution serial-section EM. We reconstructed full bodies of three larvae, before, during, and immediately after the birth of post-embryonic motor neurons, and three partial bodies at earlier and later time points. From these datasets, we reconstituted anatomical events of post-embryonic motor circuit maturation, spanning neurogenesis, neurite outgrowth, synapse formation, and synapse disassembly.

These events imply three main strategies. One is sequential remodeling of motor neurons. When the motor circuit undergoes remodeling along the body, similar motor output from juvenile and adult wiring ensures continuity of bending. Second is preparatory remodeling, where motor neurons initiate structural changes that anticipate adult-stage wiring before the juvenile configuration is dismantled; this allows a seamless transition with flexible timing. Third is communicative remodeling, where motor neurons that swap wiring partners transiently interact before the exchange occurs. These physical interactions work in conjunction with intrinsic programs to coordinate wiring replacement.

We propose that gradual structural transition helps maintain a uniform motor pattern throughout post-embryonic development. We discuss key findings in historical contexts and broad implications for how circuits accommodate structural changes.

RESULTS

Post-embryonic motor circuit development does not disrupt motor output

We asked whether post-embryonic expansion and remodeling disrupts motor output. Post-embryonic motor neurons are born between mid-L1 and early-L2.[2] When these neurons begin to integrate into the motor circuit was unknown. We thus quantified undulatory movements at multiple time points after motor neuron birth. Dorsoventral undulatory patterns are maintained across ages (Figures 1C and 1D), and bending wave propagation spatially and temporally correlated with waves of muscle calcium signals (Figures 1C and 1D). Thus, a developing larva maintains its motor output during post-embryonic development.

Deducing post-embryonic motor circuit maturation by EM reconstruction

An overview on datasets and analyses

The birth order of motor neurons was first observed by tracking nuclei.[2] Starting at mid-L1 and ending at early L2, thirteen precursor (P) cells sequentially migrate into the ventral nerve cord, divide, and give rise to new motor neurons in an anterior-to-posterior order (Figure 2A). When these motor neurons start to extend neurites and make synapses was unknown.

We reconstructed the full bodies of three larvae aged between L1 and L2 stages (Figure 2B). These datasets captured motor circuit development before (early L1, 0–1 h), during (late L1, 15 h), and after (L1/L2 transition, 16 h) the birth of post-embryonic motor neurons. The anterior nerve cords of another early L1 prior to post-embryonic neurogenesis (1–5 h) was reconstructed in another study.[11] To capture completion of remodeling, we reconstructed the anterior nerve cords of two older larvae at early L2 (18 h) and late L2 (23 h) (Figure 2C; Data S1).

Because members of the same neuron class are born sequentially (Figure 2A), by comparing motor neurons in the same class and comparing the same motor neurons at sequential stages of development, we deduced a sequence of cellular events that occur in a stereotyped and iterated manner. These observations reveal an organized orchestration of rewiring that leads to an adult-like wiring pattern by the end of the second larva stage.

Below, we describe post-embryonic remodeling through three parallel events: neurite development (Figures 2 and 3; Videos S1, S2, and S3), remodeling of the dorsal bending circuit, and building of the ventral bending circuit (Figures 4 and 5; Videos S1, S2, and S3). This categorization is an arbitrary demarcation of an organic developmental process, adopted for simplicity of presentation.

Post-embryonic neurite development of the dorsal and ventral nerve cords

In the newborn L1, the embryonic DD iMNs do not fully cover the dorsal and ventral nerve cords, but neurites from each DD neuron make at least one physical contact with neighboring DD neurons. After birth, they continue to extend neurites along both nerve cords. By late L1, all neurites are fully extended, tiling both cords with gap junctions between neighboring neurites (Figure S3A; Data S2).

In the newborn L1, the embryonic DA and DB eMNs have fully covered both dorsal and ventral nerve cords. Neurites from neighboring members of the same class overlap. These overlaps, first observed in adults and proposed to facilitate coordination of bending across body regions,[15,16,18] are maintained during their extension throughout post-embryonic stages. Motor neurons precursors (P cells) have extended cellular processes that line the ventral side of the ventral nerve cord as epidermis (Figure S1A). These processes precede sequential nuclei descent later an anterior-to-posterior temporal order.[3,8] After

(B) A dorsal view of nuclei of motor neurons or their precursors (P0–12) reconstructed by EM at three developmental time points. P1–12 reside laterally at birth and sequentially migrate into the ventral nerve cord and divide following an anterior-to-posterior order.
(C) Skeletal reconstruction of embryonic and post-embryonic motor neurons at respective developmental ages. Circles: neuron soma scaled to nuclei size; lines denote neurites.
(D) Examples of stereotyped morphology of post-embryonic motor neurons undergoing neurite outgrowth at the L1/L2 transition.
(E) Schematics summarizing the temporal order of post-embryonic motor neuron neurogenesis and neurite outgrowth.
See also Figures S1 and S2, Video S1, and Data S1, S2, S3, S4, S5, S6, and S7.

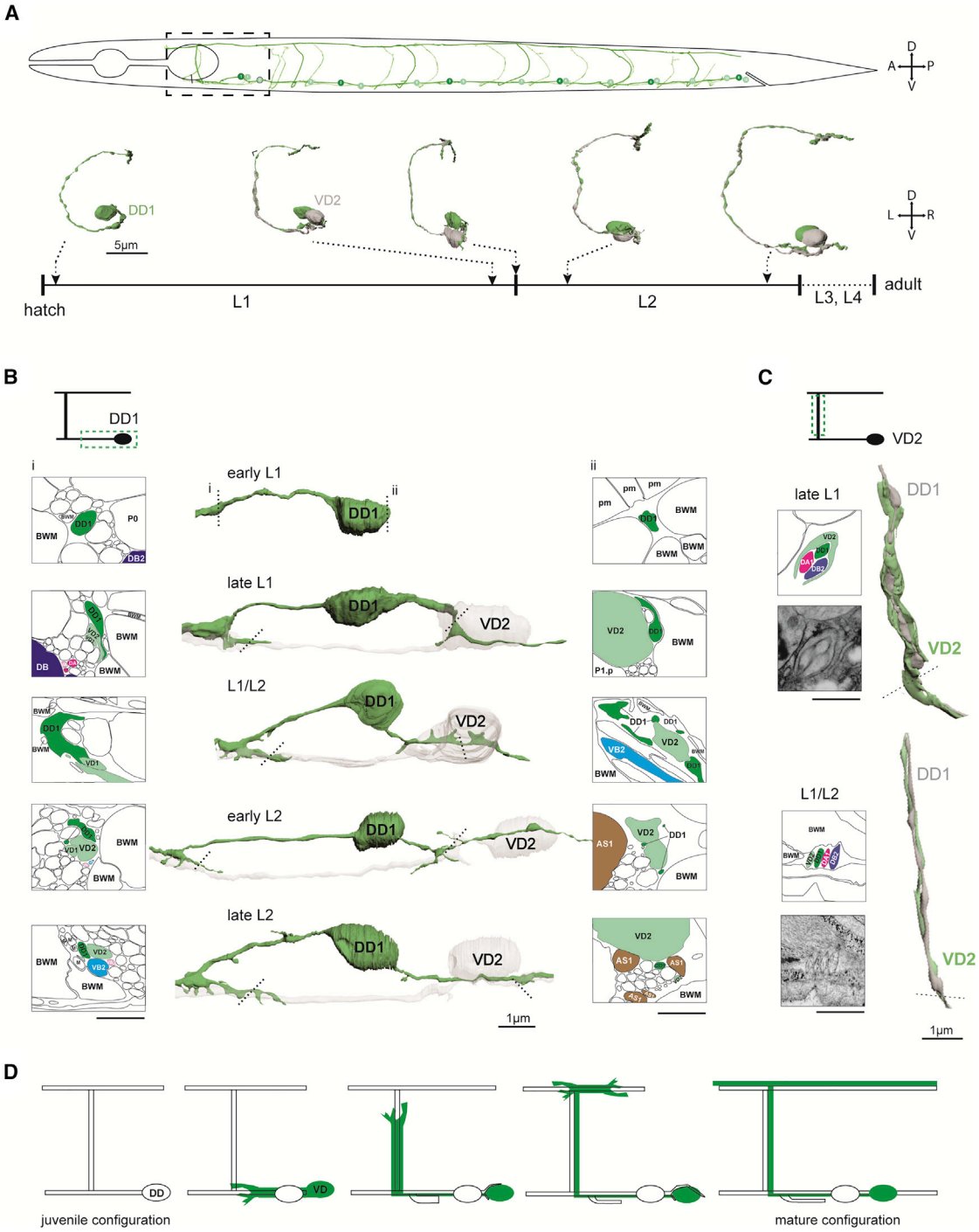

Figure 3. Neurites of embryonic and post-embryonic iMNs transiently interact

(A) (Upper) Skeleton segmentation of the DD and VD motor neurons at the L1/L2 transition. DD1 and VD2 represent their respective classes at later time points. (Lower) A tilted posterior-to-anterior view of the DD1/VD2 pair at five developmental stages.

(B) (Center) Enlarged views of migrating DD1 and VD2 neurites, with EM profiles at denoted position.

(C) Growth of VD2 commissure.

(D) Schematics summarizing transient interactions between embryonic and post-embryonic neurites.

See also Figure S3 and Video S1.

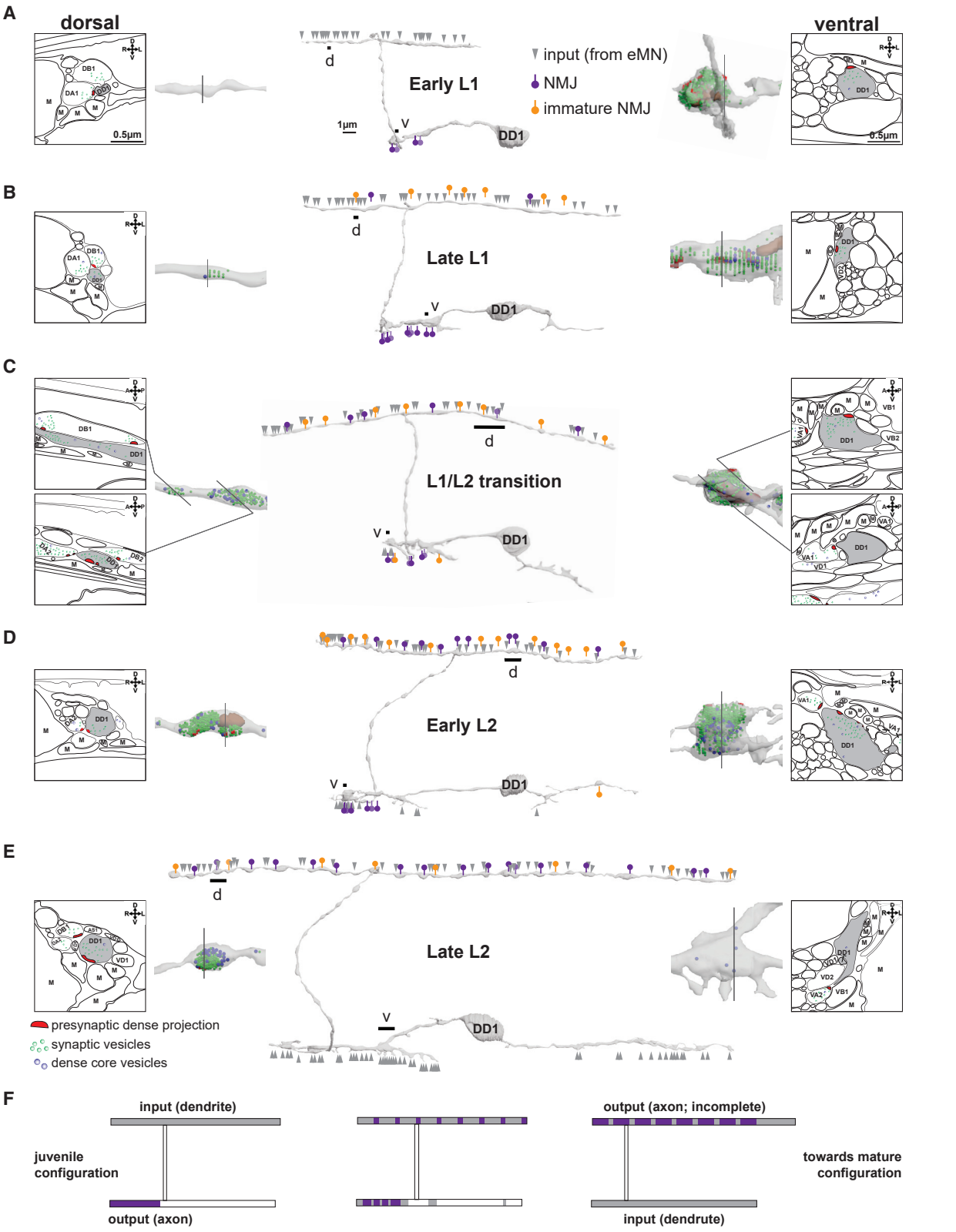

Figure 4. Synaptic rewiring of embryonic iMNs builds a new dorsal bending circuit

(A–E) Volumetric reconstruction of DD1 across developmental ages. (Center) Full models, with enlarged views of a portion of the dorsal (left) and ventral (right) processes and example EM profiles. Gray arrowheads: synaptic input to DD1; purple arrows: synaptic output from DD1 (NMJs or polyadic synapses); orange

(legend continued on next page)

entry into the cord, each nucleus divides and gives rise to post-embryonic motor neurons in a distributed manner. Most P cells contribute to one member for each motor neuron class (Figures 2A and 2B; Figure S1B).

After their birth, post-embryonic motor neurons extend neurites along the ventral nerve cord. Two (VA and VB) develop only ventral processes; two (AS and VD) also extend commissures that project dorsally and run along the dorsal nerve cord (Data S2). One class (VC), consistent with previous report,[19] does not extend neurites in our datasets.

All neurite outgrowth follows a similar process (Figure S2; Data S2–S7). They extend with a sheet-like leading edge reminiscent of growth cones,[20,21] similar to observations from motor neurons during embryogenesis[22] and VD fluorescent imaging.[23] They wrap around existing tissues, detach, and leave behind a mature nerve fiber that runs in parallel to the initial support (Figures 3C and 3D).

Some tissues interact with all members of the same neuron class, making them potential guideposts. Along the dorsal and ventral cords, extending neurites wrap or attach to epidermis and embryonic motor neuron processes (Figures S3A–S3C; Data S3–S7). Dorsal-extending commissures wrap or attach to the sublateral nerve cords, excretory canal, and embryonic motor neuron processes (Figures S3H and S3I; Data S3–S5).

Orchestrated establishment of new dorsal bending and ventral bending subcircuits

Full maturation from the L1 to adult wiring configuration requires embryonic motor neurons to establish new synaptic connections with post-embryonic motor neurons. These connections serve two purposes: adding a new circuit for ventral bending and reconstructing the circuit for dorsal bending.

To form the ventral bending circuit, embryonic iMNs (DD) disconnect from their presynaptic partners, the embryonic eMNs (DA and DB), and build new input connections from post-embryonic eMNs (VA and VB). DD iMNs further switch post-synaptic partners from the ventral to dorsal muscles. VA and VB eMNs form excitatory neuromuscular junctions (NMJs) to ventral muscles; their activation simultaneously activates DD to relax dorsal muscles, producing a ventral bend (Figure 1B).

Concurrently, the post-embryonic VD iMNs rebuild the dorsal bending circuit. VD neurons establish input connections from eMNs that excite dorsal muscles (DA and DB and post-embryonic AS) and output inhibitory NMJs to ventral muscles. When dorsal eMNs excite dorsal muscles, they simultaneously activate VD to relax ventral muscles, producing a dorsal bend (Figure 1B).

We found that remodeling events are iterated along the body by neurons of each class. In the anterior body, the embryonic and post-embryonic iMNs, DD1, and VD2, lead to rewiring (Figure 3A). Below, we describe three representative morphological events, with DD1 and VD2 as an example (Videos S1, S2, and S3).

Embryonic and post-embryonic iMNs transiently interact, coinciding with initiation of synaptic remodeling

Developing DD1 and VD2 neurites interact transiently in both dorsal and ventral cords (Figure 3; Figure S3; Video S1).

In the newborn L1, DD1 has an unbranched anteriorly projecting axon in the ventral cord and a dendrite in the dorsal cord. By the end of L1, the DD1 axon acquires two posterior-projecting branches. One projects from the soma and finishes tiling with the neighboring DD2 axon. During outgrowth, it wraps around the VD2 soma, unwrapping by the end of L2. The other projects posteriorly from the axon's proximal end, contacts the VD2 neurite, and then runs alongside it (Figure 3B).

After running alongside the juvenile DD1 axon in the ventral cord, VD2's ventral process develops a commissure that climbs dorsally by wrapping around a fascicle of commissures of embryonic motor neurons (Figure 3C). When it reaches the dorsal cord, it bifurcates, extending both posterior and anterior projections by wrapping neurites of DD1 and another neuron named RID (Figure 3D).

Along the dorsal and ventral cords, DD1 and VD2's transient physical interactions are recapitulated by other members (Figures S3B and S3C; Data S3 and S4). As there are more VD neurons, each DD neurite is wrapped by multiple VDs. Commissural interaction between VD2 and DD1 is an exception, with other VD commissures wrapping other structures.

Physical interactions in dorsal and ventral cords may provide mutual cues for wiring replacement. The VD neurites already adopt appropriate positions in both cords as they extend. In the ventral cord, they develop presynaptic termini in areas initially inhabited by DD NMJs. In the dorsal cord, they take over DD's input from embryonic eMNs as they extend (see below).

Embryonic iMNs reverse axon-dendrite identity, building the ventral bending circuit with new partners

In the newborn L1, DD's ventral process is axonal, making inhibitory NMJs to ventral muscles. DD's dorsal process is dendritic, receiving input from embryonic dorsal eMNs. In adults, the ventral process becomes the dendrite, receiving input from post-embryonic eMNs, and the dorsal process becomes the axon, making inhibitory NMJs to dorsal muscles (Figure 4; Figure S4). The striking feature is that this reversal does not involve breakdown of embryonic neurites. Instead, existing neurites undergo re-assignment of axonal and dendritic identities.[10,17,24]

At birth, the DD1 dendrite is post-synaptic to the axons of embryonic eMNs in the dorsal cord (Figure 4A; Figure S5A, *d* and *e*). Beginning in late L1, it gradually acquires presynaptic morphology. Nascent presynaptic termini appear, first as small swellings with a few vesicles (Figure 4B; Figures S5B, *g*; S5C, *i*). As the larva grows, these swellings acquire presynaptic dense projections and increase in size and number. Almost every emerging presynaptic terminal apposes a muscle arm (Figures 4C–4E; Figures S5B, *f*, and S5C, *h*).

arrows: immature presynaptic termini. EM panels showed synaptic vesicles (green), dense core vesicles (blue), presynaptic dense projections (red), and mitochondria (brown).

(F) Schematics summarizing sequential events of DD rewiring.

See also Figures S4 and S5, Video S2, and Data S8.

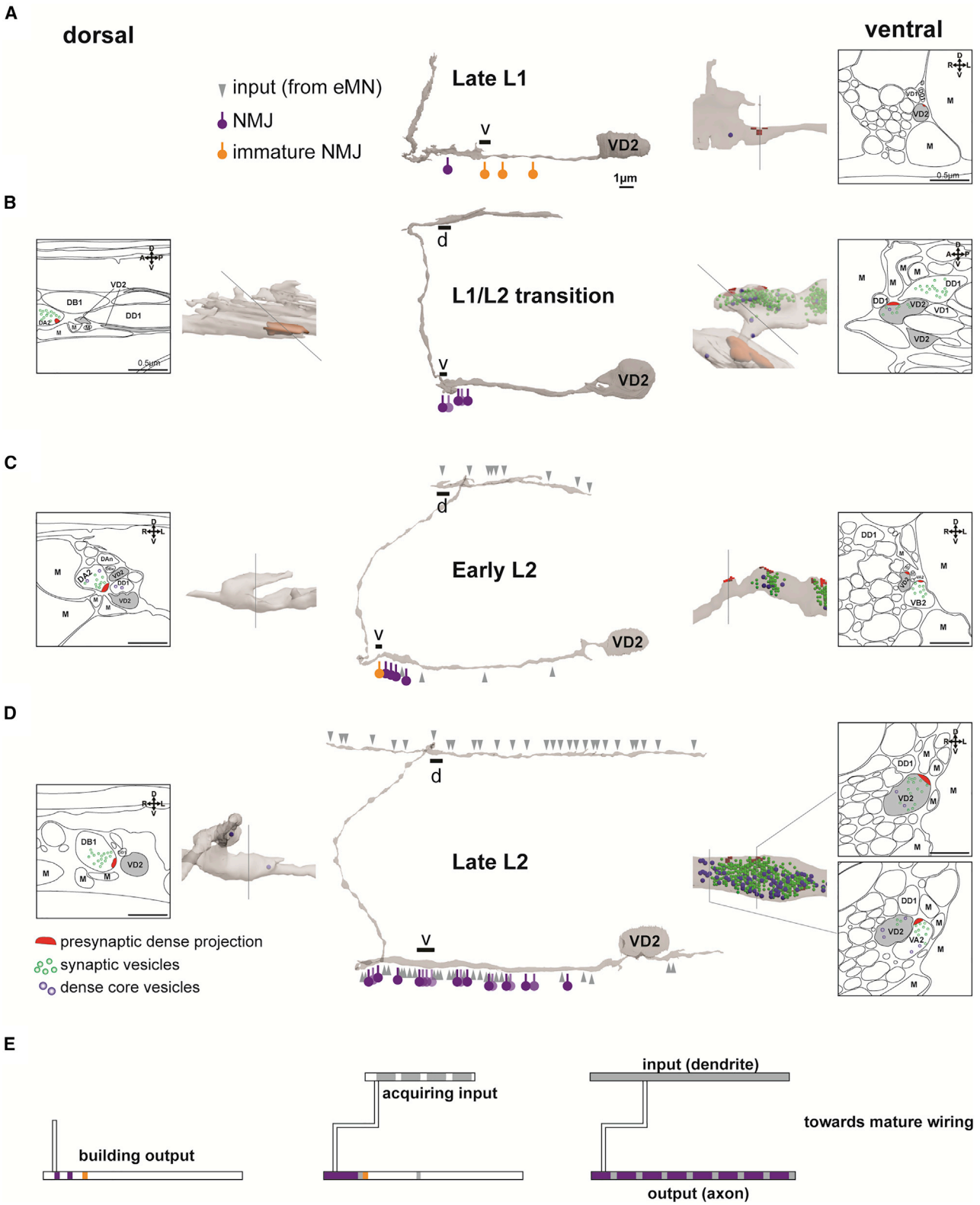

Figure 5. Post-embryonic iMNs take over embryonic iMN partners to build the ventral bending circuit

(A–D) Volumetric reconstruction of VD2 across developmental ages. (Center) Full models of VD2, with enlarged views of a portion of the dorsal (left) and ventral (right) processes and example EM profiles. Gray arrowheads: synaptic input to VD2; purple arrows: synaptic output from VD2 (NMJs or dyadic synapses); orange

(legend continued on next page)

In the ventral cord, the DD1 axon begins to exhibit post-synaptic morphology by late L1 (Figure 4B). It starts by sending spine-like structures toward swellings of extending ventral eMNs (Figure 3B; Figure S3C, *f*). By the L1/L2 transition, its anterior region apposes the maturing presynaptic termini from these eMNs (Figure 4C). As it elongates, it receives more inputs and develops more dendritic spines (Figures 4D and 4E).

Before wiring remodeling is complete, both the dorsal and ventral DD1 neurites simultaneously exhibit axonal and dendritic features. During the L1 stage, the anterior DD1 ventral process increases NMJ numbers to support its role as a juvenile axon (Figures 4A–4D). As DD1's dorsal process develops presynaptic termini, the same neurite retains apposition to presynaptic termini from the embryonic dorsal eMNs, to support its role as the juvenile dendrite (Figures 4A–4D). We only observed the disappearance of NMJs from the ventral process after many mature-looking NMJs form along the dorsal process (Figure 4E). At this stage, the dorsal process remains at the post-synaptic fields of DA and DB NMJs, although these synapses might not remain functional (see Discussion). Other DD iMNs remodel in a similar fashion to DD1.

In summary, neurites of embryonic DD iMNs undergo a gradual switch of axon-dendrite identity as they rewire. Both neurites exhibit mixed axon-dendrite morphologies during this transition. Juvenile NMJs are only dismantled after the adult-stage connectivity is fully formed (Figure 4F; Video S2).

Post-embryonic iMNs rebuild the dorsal bending circuit, replacing embryonic iMNs as neurites extend

As the embryonic DD iMNs rewire, the post-embryonic VD iMNs take over their former pre- and post-synaptic partners to make a new dorsal bending circuit (Figures 5 and S6). The striking feature of this process is that post-embryonic neurons build synapses during neurite outgrowth (Figure 5E and Video S3).

Shortly after its birth, VD2 grows an anterior-projecting process along the ventral cord. It forms nascent presynaptic terminals toward ventral muscles as it extends (Figure 5A). These immature synaptic swellings contain presynaptic dense projections but few or no vesicles (Figure 5A). They first appear near NMJs from the DD1 axon; as the larva grows, they acquire vesicle pools and increase in size, making morphologically mature NMJs to the ventral muscles (Figures 5B–5D).

The VD2 neurite next turns dorsally and joins the dorsal cord. As it extends, it intercepts the post-synaptic fields of embryonic eMNs—its synaptic partners in the adult configuration (Figures 5C and 5D). Targeting the extending VD2 neurite to its post-synaptic location might be facilitated by DD1 and RID: all VD neurites wrap them during extension (Data S4). Growing neurites of the AS eMNs, the only post-embryonically born presynaptic partner of VD's dorsal neurite, similarly wrap DD and RID neurites in the dorsal cord (Figure S7).

In early L1, DD dorsal neurites are post-synaptic to embryonic dorsal eMNs. As the larva grows, VD2's dorsal process gradually replaces DD1 in this apposition (Figure 5; Figure S7). Thus, when the dorsal eMNs contract dorsal muscles, the VD iMNs take over DD's role in relaxing ventral muscles during dorsal bends.

It is striking that the axonal fate of VD's growing process emerges before its dendrite is formed. These are not unique characteristics for iMNs: the developing neurites of all post-embryonic eMNs exhibit similar events that anticipate future wiring, although they began synaptogenesis later than nearby iMNs (Figure S7).

These observations imply that the wiring of post-embryonic motor neurons is at least partly intrinsically programmed. Physical interactions between post-embryonic and embryonic neurons might facilitate wiring maturation but are not essential.

The expression pattern of post-synaptic receptors corroborates the iMN wiring transition

Serial EM reconstruction identifies synapses by morphological features within presynaptic terminals. Because many synapses lack striking morphological features at post-synaptic sites,[25] post-synaptic partners are often identified by their physical proximity to presynaptic structures.[14,15,26] Our characterization of the motor circuit remodeling process is contingent on proximity-based synapse annotation.

To further verify our observations, we examined developmental changes of post-synaptic receptors at iMN NMJs. UNC-49 is the ionotropic $GABA_A$ receptor[27] of muscle cells.[28–30] Using an endogenously tagged UNC-49 reporter,[31] we evaluated the consistency between its localization with the change of embryonic iMN's post-synaptic partners (Figure 6A).

Consistent with earlier reports,[32] endogenous $GABA_A$ receptors were present only along the ventral cord in early L1 (Figures 6B and 6C). They appeared as six distinct and spatially segregated clusters, in correspondence to post-synaptic fields of clustered NMJs at the anterior axon of DD1–6 in EM reconstruction (Figure 4A).

At late L1, ventral $GABA_A$ clusters remained prominent. Weak signals first appeared in the anterior dorsal cord. By late L2, ventral clusters remained prominent and more evenly distributed, whereas dorsal signals also increased in intensity and spread but remained significantly weaker than ventral signals (Figures 6B and 6C).

Emergence of dorsal clusters while maintaining prominent ventral clusters is temporally consistent with the ultrastructure of rewiring iMNs: when post-embryonic iMNs begin to build NMJs along the ventral cord, embryonic iMNs maintain their NMJs to ventral muscles. Concurrently, embryonic iMNs begin to build NMJs to dorsal muscles.

DISCUSSION

The *C. elegans* motor circuit undergoes significant structural changes after hatching.[11,33–35] We describe strategies that allow the motor circuit to change its structure but preserve the motor pattern (Figure 7). Our observations confirm and extend insights from previous electron microscopy,[10] light microscopy,[17,23,32,36] and molecular studies.[37–39]

arrows: immature presynaptic termini. EM panels showed synaptic vesicles (green), dense core vesicles (blue), presynaptic dense projections (red), and mitochondria (brown).

(E) Schematics summarizing sequential establishment of VD wiring.

See also Figure S6, Video S3, and Data S8.

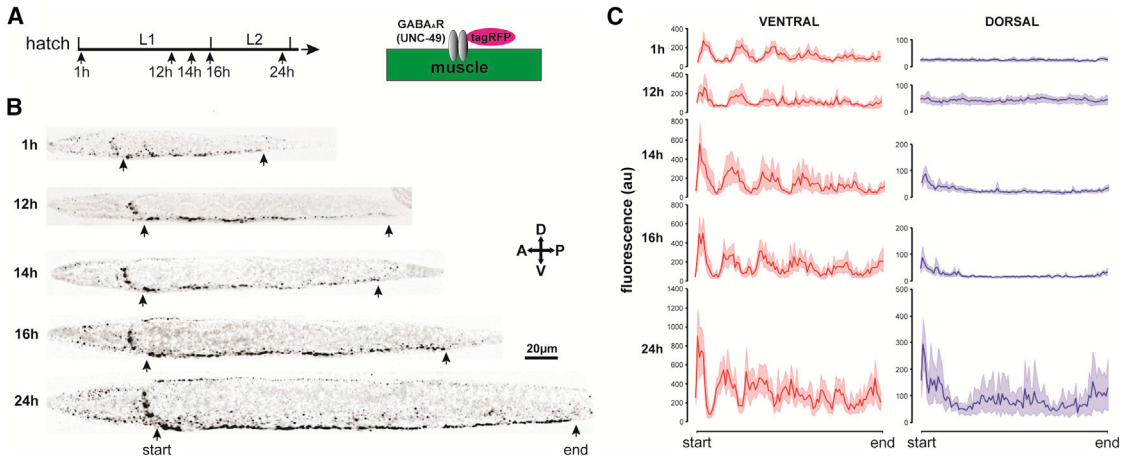

Figure 6. Post-synaptic receptor clustering corroborates with iMN morphological rewiring

(A–C) Schematics of endogenously tagged $GABA_A$ receptors (A), with examples (B) and quantification (C) of $GABA_A$::TagRFP signals at different developmental ages. Lines and shades denote the mean and standard deviation of signals, respectively.

Maturation generates symmetry

C. elegans is born with an asymmetrically wired motor circuit. Motor neurons of newborn L1 larvae are wired to contract dorsal muscles through eMNs and simultaneously relax ventral muscles through iMNs, thus promoting dorsal bending. Ventral bending occurs through extrasynaptic excitation of ventral muscles that entrain them to the activity of the dorsal bending circuit.[10,11] In contrast, the adult motor neurons form two subcircuits that separately drive dorsal and ventral bending.[14,16,18] Post-embryonic rewiring builds symmetry.

A coordinated and gradual transition

Post-embryonic motor neuron birth begins in mid-L1 and completes by early L2.[2] However, neurite extension and wiring maturation gradually continue throughout larval stages. Post-embryonic neurite outgrowth may involve physical guidance from embryonic motor and interneurons, and other guideposts (Data S3–S7). Along the nerve cords, post-embryonic neurites follow embryonic neurites of similar neuron class, such as the cholinergic neurons (PVC) for eMNs and GABAergic neurons (AVL, DD) for iMNs. Potential guideposts might work in concert with known chemical cues.[40,41]

Conversion from the L1 to adult configuration recapitulates the sequence of motor neuron birth order (Figure 7A). Across remodeling, the juvenile dorsal bending circuit remodels its wiring region by region along the body. iMNs are recruited to the ventral bending circuit, establishing input connections with ventral eMNs and new inhibitory output connections to dorsal muscles. Meanwhile, post-embryonic iMNs take over their role in the dorsal bending circuit (Figures 7B and 7C).

Functional replacement of the juvenile dorsal bending circuit by separate dorsal and ventral circuits requires precise temporal and spatial orchestration. One potential mechanism is intrinsic, preparatory rewiring. Embryonic inhibitory neurons build structures for the adult circuit while continuing to serve their role in the juvenile circuit. Another potential mechanism is extrinsic, communicative rewiring. Embryonic motor neurons may serve as guideposts to place neurites of post-embryonic motor neurons that later take over their circuit function. Points of physical contact between the embryonic and post-embryonic iMNs are where the embryonic eMNs initiate post-synaptic partner exchange. These mechanisms allow a seamless transition from the newborn to the adult circuit with structural and functional symmetry (Figure 7C).

Reversing axon-dendrite polarity

Rewiring of the embryonic iMNs disconnects them from the dorsal bending circuit and brings them into the ventral bending circuit. This transformation happens gradually (Figure 7B). First the dorsal process builds nascent presynaptic structures while retaining its juvenile dendrites. The ventral process begins to acquire input from newly born ventral eMNs while retaining its juvenile NMJs to ventral muscles. Embryonic motor neurons only dismantle juvenile connectivity after the adult circuitry is morphologically mature.

These neurites reverse polarity without retraction or relocation. Non-destructive polarity reversal implies compartmentalization and accommodation of axonal and dendritic properties in the same neurite. Unipolar and pseudo-unipolar neurons that intercalate axonal and dendritic regions are found in many species.[15,42,43] Re-assignment of axonal and dendritic compartments might be achieved by manipulation of intracellular transport. Indeed, multiple kinases that play general roles in cell polarity restrict presynaptic machineries to DD axons.[44–47] Blocking microtubule dynamics[48] or removing an ER-nuclei protein[49] blocks axon-dendrite reversal.

Uncoupling structure and functional rewiring

During axon-dendrite reversal, DD neurites exhibit mixed anatomic features. These intermediate states imply a potential requirement to uncouple synaptic wiring's structural and functional transition. For example, when mature NMJs are present in both dorsal and ventral neurites, simultaneous inhibitory input to dorsal and ventral muscles would interfere with bending wave

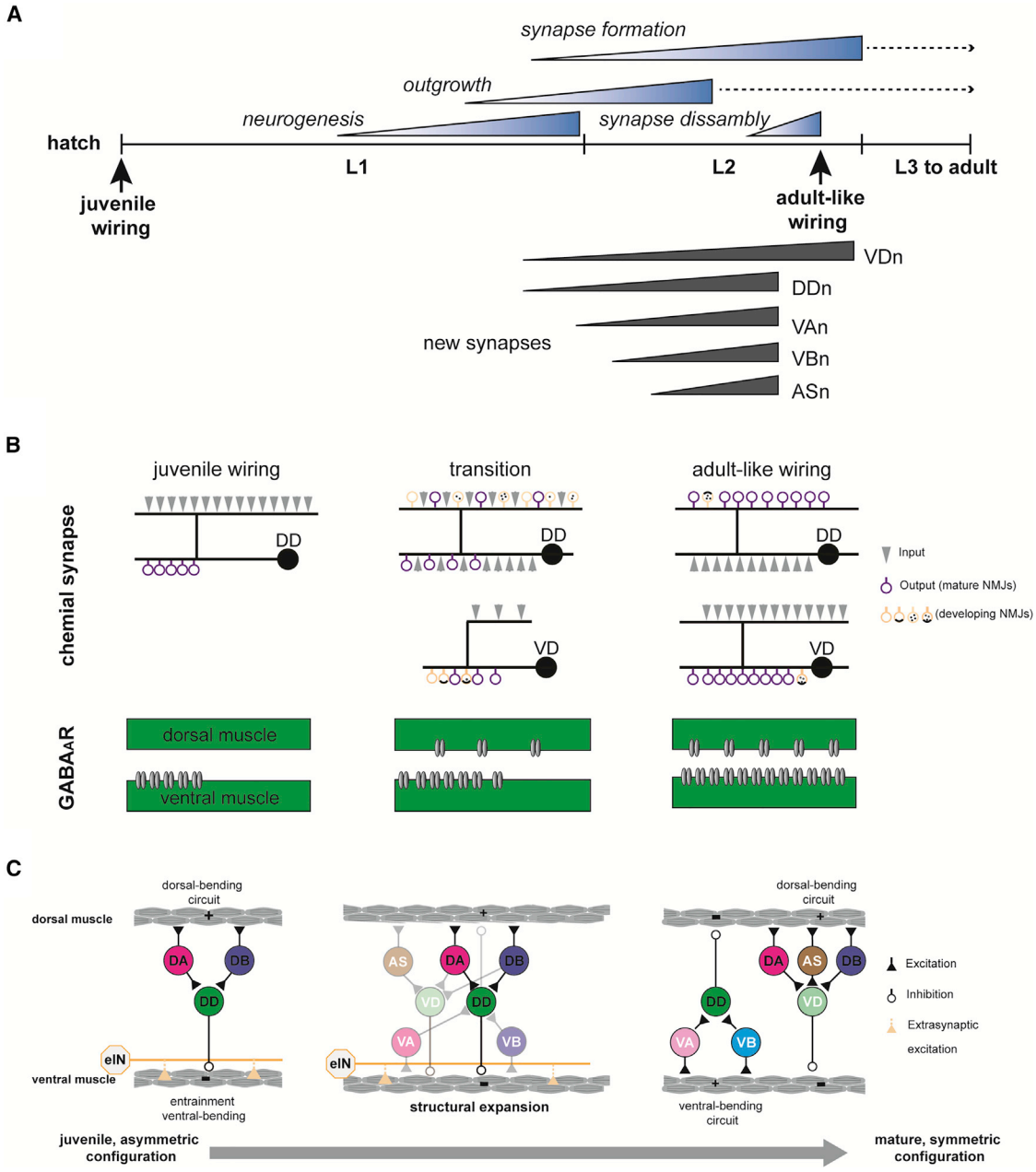

Figure 7. A summary of post-embryonic motor circuit maturation

(A) Staggered developmental timelines for anatomic events of motor circuit maturation. Above the timeline denotes periods of developmental events. Below the timeline denotes periods of transition to adult wiring by neuron class. Adult-like wiring: a state where immature synapse structures are still observed. Dashed lines: continued neurite elongation and synapse addition.

(B) (Upper) Rewiring of embryonic inhibitory motor neuros involves switch of the axon and dendrite. DD and VD build new NMJs sequentially with opposite orders. New connectivity is built before juvenile connectivity is disassembled. (lower) Post-synaptic receptors for iMN follow the pattern of morphological NMJ remodeling.

(C) *C. elegans* motor circuit acquires structural and functional symmetry through post-embryonic development. (Left) Motor neurons of juvenile animals are wired as a dorsal bending circuit. (Center) Embryonic motor neurons form new wirings with post-embryonic neurons (white letters) and may physically guide their replacement. New circuitry is built while juvenile connections are retained and functional (dark arrows). (Right) After the juvenile connectivity is disassembled, two separate subcircuits drive dorsal and ventral bending.

See also Figure S7 and Videos S1, S2, and S3

propagation. Similarly, when their dorsal and ventral processes simultaneously oppose excitatory presynaptic termini of the juvenile and adult partners, indiscriminate activation would disrupt bending wave propagation.

However, we did not observe these disruptions. Both issues could be solved by uncoupling functional and structural wiring. To prevent simultaneous relaxation of dorsal and ventral muscles, GABA reception by dorsal muscles may remain weak or DD's dorsal NMJs remain functionally silent until remodeling is complete. Similarly, DD's ventral process may have weak reception from post-embryonic eMNs or the post-embryonic motor neurons functionally silence their synapses. In both scenarios, the juvenile configuration might remain dominant until the juvenile NMJs are removed.

Intrinsic programs with flexibility

Temporal and spatial orchestration of post-embryonic motor circuit maturation implies that many events are intrinsically programmed.

Growing neurites of post-embryonic neurons initiate synapse development with their future partners as they extend. Embryonic and post-embryonic motor neurons rewire and wire, at a gross level, independently. For example, when post-embryonic iMNs innervate dorsal, instead of ventral muscles, embryonic iMNs still remodel to innervate dorsal muscles in adults.[50] When all post-embryonic motor neurons are absent,[10,51] embryonic iMNs still remodel to innervate dorsal muscles.[10] Conversely, when all embryonic iMNs are absent, post-embryonic motor neurons still innervate ventral muscles.[24,50]

Some aspects of embryonic motor neuron remodeling require post-embryonic motor neurons. In the absence of post-embryonic motor neurons, adult DD dorsal processes make NMJs to dorsal muscles but maintain post-synaptic input from the L1 circuitry, presumably due to the absence of anticipated partners.[10] An adhesive molecule promotes post-synaptic receptor clustering in DD's remodeling dendrite and maintenance[52,53] of dendritic spines.[54] The molecule is required in cholinergic motor neurons,[52] thus their adult input partners might be involved.

Intrinsic programming does not preclude flexibility during rewiring. By visualizing embryonic iMNs with fluorescent synapse markers, many genes were found to alter the timing of rewiring.[37,38] Mutants that either accelerate or delay global post-embryonic development similarly alter the timing of rewiring.[17] Without post-embryonic neurons, embryonic motor neurons delay their switch to innervate dorsal muscles[17] and maintain juvenile input.[10] Rewiring might also be delayed with reduced synaptic transmission or be accelerated with increased vesicle release.[55–57]

Physical communication and neuronal activity might be facilitatory, fine-tuning the motor neuron's intrinsic programs for coordination, flexibility, and adaptability.

Robustness of a developing motor circuit

The L1 motor circuit, resembling half of the adult motor circuit, generates an adult-like motor pattern. It compensates the absence of the ventral bending circuit with extrasynaptic signaling that entrains the ventral muscles to the activity of the dorsal bending circuit.[11] With an adult-like motor pattern in place before the adult motor circuit develops, a gradual and orchestrated replacement of juvenile wiring can occur along the body without causing changes to motor patterns. This might explain how genetic mutants that alter the timing of remodeling can nevertheless maintain an undulatory motor pattern. Ensuring the continuity of motor function during structural changes lends robustness to a motor circuit, which benefits survival in the presence of genetic and environmental adversity.

Why does it remodel?

If the basic motor pattern does not change, why remodel? Post-embryonic growth implicates a delayed maturation of the *C. elegans* motor circuit. This delay may reflect a developmental decision constrained by anatomy. Driven by its small size and short life cycle, an embryo might have prioritized the development of its central nervous system. With a functional solution for the half motor circuit at birth,[11] its negative impact on motility is minimized. However, the juvenile motor circuit likely offers only a temporary solution.[11] Control of complex postures, velocity, and direction[58–60] may require a mature motor circuit.

Different approaches by the head and the body

The *C. elegans* central and peripheral nervous systems take different approaches to reach maturity. The anatomy of head neural circuits is largely mature at birth. Wiring simply expands on a maintained topology of neuropil and may support a maturing and adaptive behavioral repertoire.[26] The body on the other hand strives to maintain the motor pattern, whereas its anatomy dramatically expands and wiring remodels. Different structural-functional relationships serve different ecological needs. These needs drive diverse approaches for plasticity or robustness in underlying circuits.

STAR★METHODS

Detailed methods are provided in the online version of this paper and include the following:

- KEY RESOURCES TABLE
- RESOURCE AVAILABILITY
  - Lead contact
  - Materials availability
  - Data and code availability
- EXPERIMENTAL MODEL AND SUBJECT DETAILS
- METHOD DETAILS
  - The age of a larva
  - Muscle calcium imaging in crawling larva
  - Swimming
  - Serial-section electron microscopy
  - Fluorescent microscopy of endogenous UNC-49::tagRFP signaling
- QUANTIFICATION AND STATISTICAL ANALYSIS

SUPPLEMENTAL INFORMATION

Supplemental information can be found online at https://doi.org/10.1016/j.cub.2022.09.065.

ACKNOWLEDGMENTS

We thank the Schafer and Bessereau labs for strains; J. White for comments; A. Cardona for CATMAID; and the Human Frontier Science Program, National

Science Foundation (US), National Institute of Health (US), Silvio Conte Center, Harvard University, Sinai Health System, and Canadian Institute of Health for funding.

AUTHOR CONTRIBUTIONS

M.Z. conceptualized and supervised the study with B.M., D.K.W., A.D.T.S., and J.W.L; B.M., D.K.W., J.M., R.S., D.H., A.D.C., and M.Z. generated, analyzed, and interpreted data; D.R.B., Y.W., Y.L., and T.A. developed tools; B.M. and M.Z. wrote the paper; and A.D.T.S. and J.L. edited the paper.

DECLARATION OF INTERESTS

The authors declare no competing interests.

Received: April 20, 2022
Revised: July 28, 2022
Accepted: September 26, 2022
Published: October 24, 2022

REFERENCES

1. Hopkins, B., Geangu, E., and Linkenauger, S. (2017). Postnatal brain development. In The Cambridge Encyclopedia of Child Development (Cambridge University Press), pp. 563–594. https://doi.org/10.1017/9781316216491.090.
2. Sulston, J.E., and Horvitz, H.R. (1977). Post-embryonic cell lineages of the nematode, *Caenorhabditis elegans*. Dev. Biol. *56*, 110–156. https://doi.org/10.1016/0012-1606(77)90158-0.
3. Sulston, J.E., Schierenberg, E., White, J.G., and Thomson, J.N. (1983). The embryonic cell lineage of the nematode *Caenorhabditis elegans*. Dev. Biol. *100*, 64–119. https://doi.org/10.1016/0012-1606(83)90201-4.
4. Stiles, J., and Jernigan, T.L. (2010). The basics of brain development. Neuropsychol. Rev. *20*, 327–348. https://doi.org/10.1007/s11065-010-9148-4.
5. Ming, G.L., and Song, H. (2011). Adult neurogenesis in the mammalian brain: significant answers and significant questions. Neuron *70*, 687–702. https://doi.org/10.1016/j.neuron.2011.05.001.
6. Alvarez-Buylla, A., and Kirn, J.R. (1997). Birth, migration, incorporation, and death of vocal control neurons in adult songbirds. J. Neurobiol. *33*, 585–601. https://doi.org/10.1002/(SICI)1097-4695(19971105)33:5<585::AID-NEU7>3.0.CO;2-0.
7. Brenowitz, E.A., and Larson, T.A. (2015). Neurogenesis in the adult avian song-control system. Cold Spring Harb. Perspect. Biol. *7*, a019000. https://doi.org/10.1101/cshperspect.a019000.
8. Sulston, J.E., and Brenner, S. (1976). Post-embryonic development in the ventral cord of *Caenorhabditis elegans*. Philos. Trans. R. Soc. Lond. B Biol. Sci. *275*, 287–297. https://doi.org/10.1098/rstb.1976.0084.
9. Zhen, M., and Samuel, A.D. (2015). *C. elegans* locomotion: small circuits, complex functions. Curr. Opin. Neurobiol. *33*, 117–126. https://doi.org/10.1016/j.conb.2015.03.009.
10. White, J.G., Albertson, D.G., and Anness, M.A.R. (1978). Connectivity changes in a class of motoneurone during the development of a nematode. Nature *271*, 764–766. https://doi.org/10.1038/271764a0.
11. Lu, Y., Ahamed, T., Mulcahy, B., Meng, J., Witvliet, D., Guan, S.A., et al. (2022). Extrasynaptic signaling enables an asymmetric juvenile motor circuit to produce symmetric undulation. Curr. Biol. *32*, https://doi.org/10.1016/j.cub.2022.09.002.
12. Haspel, G., Deng, L., Harreguy, M.B., and Tanvir, Z. (2020). Chapter 1. Elegantly. In The Neural Control. of Movement, P.J. Whelan, and S.A. Sharples, eds. (Academic Press), pp. 3–29. https://doi.org/10.1016/B978-0-12-816477-8.00001-6.
13. Wen, Q., Gao, S., and Zhen, M. (2018). *Caenorhabditis elegans* excitatory ventral cord motor neurons derive rhythm for body undulation. Philos. Trans. R. Soc. Lond. B Biol. Sci. *373*, 20170370. https://doi.org/10.1098/rstb.2017.0370.
14. White, J.G., Southgate, E., Thomson, J.N., and Brenner, S. (1976). The structure of the ventral nerve cord of *Caenorhabditis elegans*. Philos. Trans. R. Soc. Lond. B Biol. Sci. *275*, 327–348. https://doi.org/10.1098/rstb.1976.0086.
15. White, J.G., Southgate, E., Thomson, J.N., and Brenner, S. (1986). The structure of the nervous system of the nematode *Caenorhabditis elegans*. Philos. Trans. R. Soc. Lond. B Biol. Sci. *314*, 1–340. https://doi.org/10.1098/rstb.1986.0056.
16. Chen, B.L., Hall, D.H., and Chklovskii, D.B. (2006). Wiring optimization can relate neuronal structure and function. Proc. Natl. Acad. Sci. USA *103*, 4723–4728. https://doi.org/10.1073/pnas.0506806103.
17. Hallam, S.J., and Jin, Y. (1998). lin-14 regulates the timing of synaptic remodelling in Caenorhabditis elegans. Nature *395*, 78–82. https://doi.org/10.1038/25757.
18. Hall, D.H., and Russell, R.L. (1991). The posterior nervous system of the nematode *Caenorhabditis elegans*: serial reconstruction of identified neurons and complete pattern of synaptic interactions. J. Neurosci. *11*, 1–22. https://doi.org/10.1523/JNEUROSCI.11-01-00001.1991.
19. Li, C., and Chalfie, M. (1990). Organogenesis in *C. elegans*: positioning of neurons and muscles in the egg-laying system. Neuron *4*, 681–695. https://doi.org/10.1016/0896-6273(90)90195-L.
20. Cajal, S.R. (1890). A quelle epoque apparaissent les expansions des cellules nerveuses de la moelle epiniere du poulet? Anat. Anz. *5*, 609–613.
21. Harrison, R.G. (1910). The outgrowth of the nerve fiber as a mode of protoplasmic movement. J. Exp. Zool. *9*, 787–846. https://doi.org/10.1002/jez.1400090405.
22. Durbin, R. (1987). Studies on the development and organization of the nervous system of *Caenorhabditis elegans*. Thesis (University of Cambridge).
23. Knobel, K.M., Jorgensen, E.M., and Bastiani, M.J. (1999). Growth cones stall and collapse during axon outgrowth in *Caenorhabditis elegans*. Development *126*, 4489–4498. https://doi.org/10.1242/dev.126.20.4489.
24. Walthall, W.W., Li, L., Plunkett, J.A., and Hsu, C.-Y. (1993). Changing synaptic specificities in the nervous system of *Caenorhabditis elegans*: differentiation of the DD motoneurons. J. Neurobiol. *24*, 1589–1599. https://doi.org/10.1002/neu.480241204.
25. Harris, K.M., and Weinberg, R.J. (2012). Ultrastructure of synapses in the mammalian brain. Cold Spring Harb. Perspect. Biol. *4*, a005587. https://doi.org/10.1101/cshperspect.a005587.
26. Witvliet, D., Mulcahy, B., Mitchell, J.K., Meirovitch, Y., Berger, D.R., Wu, Y., Liu, Y., Koh, W.X., Parvathala, R., Holmyard, D., et al. (2021). Connectomes across development reveal principles of brain maturation. Nature *596*, 257–261. https://doi.org/10.1038/s41586-021-03778-8.
27. Bamber, B.A., Beg, A.A., Twyman, R.E., and Jorgensen, E.M. (1999). The *Caenorhabditis elegans unc-49* Locus Encodes Multiple Subunits of a heteromultimeric GABA Receptor. J. Neurosci. *19*, 5348–5359. https://doi.org/10.1523/JNEUROSCI.19-13-05348.1999.
28. Bamber, B.A., Twyman, R.E., and Jorgensen, E.M. (2003). Pharmacological characterization of the homomeric and heteromeric UNC-49 GABA receptors in *C. elegans*. Br. J. Pharmacol. *138*, 883–893. https://doi.org/10.1038/sj.bjp.0705119.
29. Gao, S., and Zhen, M. (2011). Action potentials drive body wall muscle contractions in *Caenorhabditis elegans*. Proc. Natl. Acad. Sci. USA *108*, 2557–2562. https://doi.org/10.1073/pnas.1012346108.
30. Liu, P., Chen, B., and Wang, Z.-W. (2013). Postsynaptic current bursts instruct action potential firing at a graded synapse. Nat. Commun. *4*, 1911. https://doi.org/10.1038/ncomms2925.
31. D'Alessandro, M., Richard, M., Stigloher, C., Gache, V., Boulin, T., Richmond, J.E., and Bessereau, J.-L. (2018). CRELD1 is an evolutionarily-conserved maturational enhancer of ionotropic acetylcholine receptors. eLife *7*, e39649. https://doi.org/10.7554/eLife.39649.
32. Gally, C., and Bessereau, J.-L. (2003). GABA is dispensable for the formation of junctional GABA receptor clusters in *Caenorhabditis elegans*.

J. Neurosci. *23*, 2591–2599. https://doi.org/10.1523/JNEUROSCI.23-07-02591.2003.

33. Croll, N.A. (1975). Components and patterns in the behaviour of the nematode *Caenorhabditis elegans*. J. Zool. *176*, 159–176. https://doi.org/10.1111/j.1469-7998.1975.tb03191.x.
34. Backholm, M., Ryu, W.S., and Dalnoki-Veress, K. (2013). Viscoelastic properties of the nematode *Caenorhabditis elegans*, a self-similar, shear-thinning worm. Proc. Natl. Acad. Sci. USA *110*, 4528–4533. https://doi.org/10.1073/pnas.1219965110.
35. Fang-Yen, C., Wyart, M., Xie, J., Kawai, R., Kodger, T., Chen, S., Wen, Q., and Samuel, A.D.T. (2010). Biomechanical analysis of gait adaptation in the nematode *Caenorhabditis elegans*. Proc. Natl. Acad. Sci. USA *107*, 20323–20328. https://doi.org/10.1073/pnas.1003016107.
36. Nonet, M.L. (1999). Visualization of synaptic specializations in live *C. elegans* with synaptic vesicle protein-GFP fusions. J. Neurosci. Methods *89*, 33–40. https://doi.org/10.1016/S0165-0270(99)00031-X.
37. Cuentas-Condori, A., and Miller Rd, D.M., 3rd. (2020). Synaptic remodeling, lessons from *C. elegans*. J. Neurogenet. *34*, 307–322. https://doi.org/10.1080/01677063.2020.1802725.
38. Kurup, N., and Jin, Y. (2016). Neural circuit rewiring: insights from DD synapse remodeling. Worm *5*, e1129486. https://doi.org/10.1080/21624054.2015.1129486.
39. Howell, K., White, J.G., and Hobert, O. (2015). Spatiotemporal control of a novel synaptic organizer molecule. Nature *523*, 83–87. https://doi.org/10.1038/nature14545.
40. McIntire, S.L., Garriga, G., White, J., Jacobson, D., and Horvitz, H.R. (1992). Genes necessary for directed axonal elongation or fasciculation in *C. elegans*. Neuron *8*, 307–322. https://doi.org/10.1016/0896-6273(92)90297-Q.
41. Hedgecock, E.M., Culotti, J.G., and Hall, D.H. (1990). The unc-5, unc-6, and unc-40 genes guide circumferential migrations of pioneer axons and mesodermal cells on the epidermis in C. elegans. Neuron *4*, 61–85. https://doi.org/10.1016/0896-6273(90)90444-K.
42. Rolls, M.M. (2011). Neuronal polarity in *Drosophila*: sorting out axons and dendrites. Dev. Neurobiol. *71*, 419–429. https://doi.org/10.1002/dneu.20836.
43. Kandel, E.R., Koester, J.D., Mack, S.H., and Siegelbaum, S.A. (2021). Principles of Neural Science, Sixth Edition (McGraw Hill Professional).
44. Crump, J.G., Zhen, M., Jin, Y., and Bargmann, C.I. (2001). The SAD-1 kinase regulates presynaptic vesicle clustering and axon termination. Neuron *29*, 115–129. https://doi.org/10.1016/S0896-6273(01)00184-2.
45. Kim, J.S., Lilley, B.N., Zhang, C., Shokat, K.M., Sanes, J.R., and Zhen, M. (2008). A chemical-genetic strategy reveals distinct temporal requirements for SAD-1 kinase in neuronal polarization and synapse formation. Neural Dev. *3*, 23. https://doi.org/10.1186/1749-8104-3-23.
46. Hung, W., Hwang, C., Po, M.D., and Zhen, M. (2007). Neuronal polarity is regulated by a direct interaction between a scaffolding protein, Neurabin, and a presynaptic SAD-1 kinase in *Caenorhabditis elegans*. Development *134*, 237–249. https://doi.org/10.1242/dev.02725.
47. Park, M., Watanabe, S., Poon, V.Y.N., Ou, C.-Y., Jorgensen, E.M., and Shen, K. (2011). CYY-1/Cyclin Y and CDK-5 differentially regulate synapse elimination and formation for rewiring neural circuits. Neuron *70*, 742–757. https://doi.org/10.1016/j.neuron.2011.04.002.
48. Kurup, N., Yan, D., Goncharov, A., and Jin, Y. (2015). Dynamic microtubules drive circuit rewiring in the absence of neurite remodeling. Curr. Biol. *25*, 1594–1605. https://doi.org/10.1016/j.cub.2015.04.061.
49. Meng, J., Ma, X., Tao, H., Jin, X., Witvliet, D., Mitchell, J., Zhu, M., Dong, M.-Q., Zhen, M., Jin, Y., et al. (2017). Myrf ER-bound transcription factors drive *C. elegans* synaptic plasticity via cleavage-dependent nuclear translocation. Dev. Cell *41*, 180–194.e7. https://doi.org/10.1016/j.devcel.2017.03.022.
50. Walthall, W.W., and Plunkett, J.A. (1995). Genetic transformation of the synaptic pattern of a motoneuron class in *Caenorhabditis elegans*. J. Neurosci. *15*, 1035–1043. https://doi.org/10.1523/JNEUROSCI.15-02-01035.1995.
51. Korzelius, J., The, I., Ruijtenberg, S., Portegijs, V., Xu, H., Horvitz, H.R., and van den Heuvel, S. (2011). *C. elegans* MCM-4 is a general DNA replication and checkpoint component with an epidermis-specific requirement for growth and viability. Dev. Biol. *350*, 358–369. https://doi.org/10.1016/j.ydbio.2010.12.009.
52. Philbrook, A., Ramachandran, S., Lambert, C.M., Oliver, D., Florman, J., Alkema, M.J., Lemons, M., and Francis, M.M. (2018). Neurexin directs partner-specific synaptic connectivity in *C. elegans*. eLife *7*, e35692. https://doi.org/10.7554/eLife.35692.
53. Oliver, D., Ramachandran, S., Philbrook, A., Lambert, C.M., Nguyen, K.C.Q., Hall, D.H., and Francis, M.M. (2022). Kinesin-3 mediated axonal delivery of presynaptic neurexin stabilizes dendritic spines and postsynaptic components. PLoS Genet. *18*, e1010016. https://doi.org/10.1371/journal.pgen.1010016.
54. Cuentas-Condori, A., Mulcahy, B., He, S., Palumbos, S., Zhen, M., and Miller, D.M., III. (2019). *C. elegans* neurons have functional dendritic spines. eLife *8*, e47918. https://doi.org/10.7554/eLife.47918.
55. Thompson-Peer, K.L., Bai, J., Hu, Z., and Kaplan, J.M. (2012). HBL-1 patterns synaptic remodeling in *C. elegans*. Neuron *73*, 453–465. https://doi.org/10.1016/j.neuron.2011.11.025.
56. Miller-Fleming, T.W., Petersen, S.C., Manning, L., Matthewman, C., Gornet, M., Beers, A., Hori, S., Mitani, S., Bianchi, L., Richmond, J., et al. (2016). The DEG/ENaC cation channel protein UNC-8 drives activity-dependent synapse removal in remodeling GABAergic neurons. eLife *5*, e14599. https://doi.org/10.7554/eLife.14599.
57. Miller-Fleming, T.W., Cuentas-Condori, A., Manning, L., Palumbos, S., Richmond, J.E., and Miller, D.M. (2021). Transcriptional control of parallel-acting pathways that remove specific presynaptic proteins in remodeling neurons. J. Neurosci. *41*, 5849–5866. https://doi.org/10.1523/JNEUROSCI.0893-20.2021.
58. Bilbao, A., Patel, A.K., Rahman, M., Vanapalli, S.A., and Blawzdziewicz, J. (2018). Roll maneuvers are essential for active reorientation of Caenorhabditis elegans in 3D media *Caenorhabditis elegans* in 3D media. Proc. Natl. Acad. Sci. USA *115*, E3616–E3625. https://doi.org/10.1073/pnas.1706754115.
59. Cassada, R.C., and Russell, R.L. (1975). The dauerlarva, a post-embryonic developmental variant of the nematode *Caenorhabditis elegans*. Dev. Biol. *46*, 326–342. https://doi.org/10.1016/0012-1606(75)90109-8.
60. Lee, H., Choi, M.K., Lee, D., Kim, H.S., Hwang, H., Kim, H., Park, S., Paik, Y.K., and Lee, J. (2011). Nictation, a dispersal behavior of the nematode *Caenorhabditis elegans*, is regulated by IL2 neurons. Nat. Neurosci. *15*, 107–112. https://doi.org/10.1038/nn.2975.
61. Butler, V.J., Branicky, R., Yemini, E., Liewald, J.F., Gottschalk, A., Kerr, R.A., Chklovskii, D.B., and Schafer, W.R. (2015). A consistent muscle activation strategy underlies crawling and swimming in *Caenorhabditis elegans*. J. R. Soc. Interface *12*, 20140963. https://doi.org/10.1098/rsif.2014.0963.
62. Edelstein, A.D., Tsuchida, M.A., Amodaj, N., Pinkard, H., Vale, R.D., and Stuurman, N. (2014). Advanced methods of microscope control using μManager software. J. Biol. Methods *1*, e10. https://doi.org/10.14440/jbm.2014.36.
63. Kawano, T., Po, M.D., Gao, S., Leung, G., Ryu, W.S., and Zhen, M. (2011). An imbalancing act: gap junctions reduce the backward motor circuit activity to bias *C. elegans* for forward locomotion. Neuron *72*, 572–586. https://doi.org/10.1016/j.neuron.2011.09.005.
64. Stern, S., Kirst, C., and Bargmann, C.I. (2017). Neuromodulatory control of long-term behavioral patterns and individuality across development. Cell *171*, 1649–1662.e10. https://doi.org/10.1016/j.cell.2017.10.041.
65. Mulcahy, B., Witvliet, D., Holmyard, D., Mitchell, J., Chisholm, A.D., Meirovitch, Y., Samuel, A.D.T., and Zhen, M. (2018). A pipeline for volume electron microscopy of the *Caenorhabditis elegans* nervous system. Front. Neural Circuits *12*, 94.

66. Weimer, R.M. (2006). Preservation of *C. elegans* Tissue Via high-pressure freezing and freeze-substitution for ultrastructural analysis and immunocytochemistry. Methods Mol. Biol. *351*, 203–221. https://doi.org/10.1385/1-59745-151-7:203.

67. Schalek, R., Wilson, A., Lichtman, J., Josh, M., Kasthuri, N., Berger, D., Seung, S., Anger, P., Hayworth, K., and Aderhold, D. (2012). ATUM-based SEM for high-speed large-volume biological reconstructions. Microsc. Microanal. *18*, 572–573. https://doi.org/10.1017/S1431927612004710.

68. Hayworth, K.J., Morgan, J.L., Schalek, R., Berger, D.R., Hildebrand, D.G.C., and Lichtman, J.W. (2014). Imaging ATUM ultrathin section libraries with WaferMapper: a multi-scale approach to EM reconstruction of neural circuits. Front. Neural Circuits *8*, 68.

69. Schindelin, J., Arganda-Carreras, I., Frise, E., Kaynig, V., Longair, M., Pietzsch, T., Preibisch, S., Rueden, C., Saalfeld, S., Schmid, B., et al. (2012). Fiji: an open-source platform for biological-image analysis. Nat. Methods *9*, 676–682. https://doi.org/10.1038/nmeth.2019.

70. Cardona, A., Saalfeld, S., Schindelin, J., Arganda-Carreras, I., Preibisch, S., Longair, M., Tomancak, P., Hartenstein, V., and Douglas, R.J. (2012). TrakEM2 software for neural circuit reconstruction. PLoS One *7*, e38011. https://doi.org/10.1371/journal.pone.0038011.

71. Saalfeld, S., Cardona, A., Hartenstein, V., and Tomančák, P. (2009). CATMAID: collaborative annotation toolkit for massive amounts of image data. Bioinformatics *25*, 1984–1986. https://doi.org/10.1093/bioinformatics/btp266.

72. Berger, D.R., Seung, H.S., and Lichtman, J.W. (2018). VAST (volume annotation and segmentation tool): efficient manual and semi-automatic labeling of large 3D image stacks. Front. Neural Circuits *12*, 88.

73. Ruvkun, G., and Giusto, J. (1989). The *Caenorhabditis elegans* heterochronic gene *lin-14* encodes a nuclear protein that forms a temporal developmental switch. Nature *338*, 313–319. https://doi.org/10.1038/338313a0.

74. Miller, D.M., and Shakes, D.C. (1995). Chapter 16. Immunofluorescence microscopy. In Methods in Cell Biology *Caenorhabditis elegans*: Modern Biological Analysis of an Organism, H.F. Epstein, and D.C. Shakes, eds. (Academic Press), pp. 365–394. https://doi.org/10.1016/S0091-679X(08)61396-5.

STAR★METHODS

KEY RESOURCES TABLE

REAGENT or RESOURCE	SOURCE	IDENTIFIER
Antibodies		
RFP antibody [5F8]	Chromotek	Cat#5f8-20
Bacterial strains		
E. coli	*Caenorhabditis* Genetics Center	RRID: WB-STRAIN:OP50-1
Experimental models		
C. elegans	*Caenorhabditis* Genetics Center	RRID: N2 Bristol
	Bessereau laboratory Schafer laboratory	RRID: EN296 RRID: AQ2953
EM datasets	This study	Database: https://bossdb.org/project/mulcahy2022
	This study	Database: https://nemanode.com/
	This study	Data S1
	This study	Data S2
	This study	Data S3
	This study	Data S4
	This study	Data S5
	This study	Data S6
	This study	Data S7
	This study	Data S8
Software and algorithms		
CATMAID	Opensource	RRID: GPLv3
ImageJ	NIH Image	RRID: SCR_003070
MATLAB	MathWorks	RRID: SCR_001622
GraphPad Prism	GraphPad	RRID: SCR_002798
Codes		
Github	This study	Database: https://github.com/zhen-lab/Beta_Function_Analysis

RESOURCE AVAILABILITY

Lead contact

Further information and requests should be directed to lead contact, Mei Zhen (meizhen@lunenfeld.ca).

Materials availability

Requests for strains should be directed to the *Caenorhabditis* Genetics Center, Schafer and Bessereau labs.

Data and code availability

- Original electron micrograph data are available at bossdb.org.
- Wiring diagrams are provided in Figures 1, 7, S4 (DD1), and S6 (VD2), and nemanode.com, which is linked to wormatlas.org.
- MATLAB scripts for calcium imaging analyses are available in GitHub https://github.com/zhen-lab/Beta/_Function/_Analysis.
- Original light microscopy data are available upon request to lead contacts.

EXPERIMENTAL MODEL AND SUBJECT DETAILS

C. elegans strains were grown and maintained on nematode growth media (NGM) plates seeded with the *Escherichia coli* strain OP50 at 22.5°C. The N2 Bristol strain was obtained from the *Caenorhabditis* Genetics Center (CGC). The EN296 [*UNC-49::TagRFP*] strain[31] was obtained from the Bessereau lab. The AQ2953 (*ljIs131[Pmyo-3-GCaMP3::UrSL2::RFP]* strain[61] was obtained from the Schafer lab.

METHOD DETAILS

The age of a larva

Because the rate of developmental changes is dependent on raising temperatures, the age of larva (hours after hatching) is scaled to the lineage chart (N2 animals raised at 20°C) using established post-embryonic anatomical landmarks.[2] For electron microscopy studies, see Data S1 for main landmarks used to determine the age of larva. For the age of non-wild-type animals (muscle GCaMP::tagRFP and UNC-49::TagRFP), we scaled to the lineage chart by two landmarks: the presence and absence of L1 alae, and the number of gonad cells revealed by DIC imaging.

Muscle calcium imaging in crawling larva

Animals expressing GCaMP3 and RFP in body wall muscles[61] were synchronized, sandwiched between a 2% agarose pad and a glass coverslip. Animals were imaged using a compound fluorescence microscope equipped with a dual beam DV2 beam splitter to simultaneously record fluorescence from green and red channels. A motorized stage and custom plugin for μManager were used to track animals as they moved around the agarose pad, with a 10x objective and 10Hz sampling rate.[62,63] Our datasets (Figures 1C and 1D) did not include 1hr L1 larvae because under the coverslip, which was necessary for reducing motion artifact for these calcium imaging experiments, the newborn larvae were unable to move. Though animals undergo quiescent periods during molting,[59,64] this did not interfere with our test for the ability to locomote, as animals were in a stimulated state (picked onto an agarose pad, under a coverslip, with bright illumination) and moved anyway.

Body curvature and fluorescence intensity along the body axis were computed using custom scripts.[11] Briefly head and tail are manually assigned in the first frame of the recording and tracked afterward. The contour of the worm is divided into 100 segments along the anterior-posterior axis and further segment into the dorsal and ventral segments across the mid-line. Averaged intensity for pixels within each segment is used as proxy for the activity for this muscle segment. The phase difference was calculated by first using the Hilbert transform as implemented by MATLAB's Hilbert function to obtain an analytical representation of the signal. The difference between the phase angles obtained from the analytical representation of muscle activities and curvatures was used to generate phase difference histograms.

Swimming

For swimming assays, animals were placed in a drop of M9 on a glass coverslip, contained within a 1 cm diameter Vaseline stamp, and imaged at 10Hz on a Zeiss V16 dissecting microscope. Swim cycles were manually counted from the videos.

Serial-section electron microscopy

Animals were prepared by high pressure freezing followed by freeze substitution in acetone containing fixatives.[65,66] The freeze substitution protocol was: -90°C for 96h in 0.1% tannic acid and 0.5% glutaraldehyde; wash with acetone 4x over 4h; exchange with 2% OsO4 and ramp to -20°C over 14h; hold at -20°C for 14h; ramp to 4°C over 4h; wash with acetone 4x over 1h. Freeze substituted samples were infiltrated with Spurr-Quetol resin, embedded as single animals and cured in a 60°C oven for 24h.

The 1-5hr and 15h animals were processed for TEM: serial 50nm (1-5hr) and 70nm (15hr) sections were collected on 2x0.5mm slot grids, stained with 2% UA and 0.1% lead citrate, and imaged at 0.7-1nm/pixel resolution using a Technai T20 TEM with AMT 16000 and Gatan Orius cameras. The rest of the animals were processed for SEM: serial 30nm sections were cut collected onto kapton tape using an ATUM,[67] glued to silicon wafers, post-stained with 4% UA and Leica Ultrostain II (3% lead citrate), and semi-automatically imaged using a FEI Magellan scanning electron microscope at 1-2nm/pixel.[68]

Micrographs from TEM and SEM were stitched into 3D volumes using TrakEM2[69,70] and exported to CATMAID[71] for cell identification, skeleton tracing and connectivity mapping.[26,65] All cells were identified in all datasets and all neurites were traced through dorsal, ventral, circumferential and sub-lateral nerve cords. For all EM micrographs, identity of all membrane profiles was identified, but only annotation for cells of the motor circuit (Figure 1B), as well as neuronal and non-neuronal cells of consistent adjacency with the motor circuit neurons (e.g. muscle arms, AVL, etc.) were shown to simplify presentation in figures.

Volumetric reconstructions were performed manually in VAST[72] and the resulting 3D models were processed using Autodesk 3ds Max or Blender. The 16hr dataset was realigned for volumetric reconstruction using a custom stitching pipeline.[26]

Chemical synapse annotation of all datasets was performed manually in CATMAID,[71] similar to previously described[26,65] with minor modifications. For all datasets, chemical synapses were annotated by the lead author (BM). At ambiguous regions, a second annotator was consulted to reduce subjectivity. Criteria for mature presynapses include swellings along processes that contain at least one presynaptic dense projection (active zone) with an associated cloud of mostly clear core vesicles. Some areas of neurites contained either a dense projection, or a cloud of vesicles, but not both. These were assigned as 'immature synapses' and were largely restricted to the expected areas with ongoing synaptogenesis (e.g., the dorsal DD and ventral VD processes after the late L1 stage). Post-synaptic partners were assigned by physical adjacency to the presynaptic dense projection. Only chemical synapses were systematically annotated throughout the EM volume. Gap junctions have not been systematically annotated; examples of prominent gap junctions, annotated by closely aligned membranes with darkly stained plaques and reproducible among members of the same classes, were highlighted in Figures S3 and S7.

Fluorescent microscopy of endogenous UNC-49::tagRFP signaling

The EN296 strain contains an N-terminal insertion of tagRFP at the endogenous *unc-49* locus.[31] Antibody staining against tagRFP, which labels the A subunit, revealed the same staining pattern as using antibodies against the endogenous UNC-49 proteins.[31] To examine the endogenous UNC-49::tagRFP signaling, EN296 animals were fixed on ice with 2% paraformaldehyde and 1x modified Ruvkun's witches brew[73,74] to reduce gut autofluorescence. Fluorescence was imaged on a Nikon confocal microscope using images stacks followed by maximum intensity projections.

QUANTIFICATION AND STATISTICAL ANALYSIS

For quantification of UNC-49::TagRFP fluorescence in the ventral and dorsal nerve cords, ROIs were drawn along the nerve cords in Fiji[69] and fluorescence intensity along the body axis was plotted using a custom script that binned the ROI into 100 segments and computed mean intensity and standard deviation of each segment. No statistics were performed.